IAES International Journal of Artificial Intelligence (IJ-AI)
Vol. 13, No. 3, September 2024, pp. 3510~3522
ISSN: 2252-8938, DOI: 10.11591/ijai.v13.i3.pp3510-3522

New disturbance observer-based speed estimator for induction motor

Katherin Indriawati[1], Febry Pandu Wijaya[2], Choirul Mufit[3]
[1]Department of Engineering Physics, Institut Teknologi Sepuluh Nopember, Surabaya, Indonesia
[2]Deputi Research and Development, PT INKA, Madiun, Indonesia
[3]Department of Electrical Engineering, Universitas 17 Agustus 1945, Jakarta, Indonesia

Article Info

Article history:

Received Sep 4, 2023
Revised Oct 29, 2023
Accepted Nov 15, 2023

Keywords:

Disturbance observer
Extended state
Induction motor
Sensorless drives
Speed estimator

ABSTRACT

This paper discusses a novel disturbance observer designed as an estimator to determine the rotor speed of an induction motor. This observer is a solution to obtain a simple structure with a small number of compact observer gains. Furthermore, the adaptation law is no longer required to estimate induction motor speed values. This is a machine model-based computation method that uses a stationary reference frame. The nonlinearity problem is solved using an additional state vector in the observer model, which is known as an extended state observer. This approach easily and systematically determines the observer gain by applying the linear quadratic regulator (LQR) method, thereby avoiding time-consuming trial errors. The proposed observer, which was presented in both continuous and discrete forms, was tested using a sensorless V/f- controlled induction motor. The simulation results show that the proposed observer can accurately estimate all states, namely, the rotor flux and stator current; therefore, the proposed estimator provides the speed and electromagnetic torque for a wide operational range of speeds and load torques. It was also shown that the proposed observer was robust to noise and uncertainty in induction motor parameters.

Corresponding Author:

Katherin Indriawati
Department of Engineering Physics, Institut Teknologi Sepuluh Nopember
Surabaya 60111, Indonesia
Email: katherin@ep.its.ac.id

1. INTRODUCTION

Today, the development of modern drive systems has led to the use of speed observers as substitutes for speed sensors. A control system with a speed estimator is referred to as a sensorless system. The speed estimation method of a sensorless system can be divided into three: rotor slot harmonic, frequency signal injection, and machine model-based. The last method is known to be simpler and has a better performance at a high speed, yet it has a low accuracy at a low speed as a result of parameter variation.

The comparison between the performance of each model-based method has been reported in [1]. It is shown that the Kalman filter solves noise best among the methods. However, its dynamic behavior, complexity, and computation time are worse than the adaptive flux observer (AFO). On the other side, artificial intelligence (AI) excels at almost all criteria, but its complexity and computation time are not better than the AFO and sliding mode observer. It is shown that the observer offers a potential solution.

The observer for the induction motor speed estimator is built to estimate the state variables. The estimated state variables are the rotor fluxes flux and the stator current. Sometimes, in the estimator, the rotor speed is treated as an additional parameter instead of the estimated state variable. A good observer should be able to reconstruct these state variables with minimum steady-state errors and dynamic-state errors so that the estimator can estimate the speed accurately. The main problem that occurs in the sensorless system is the accuracy in estimating flux values with variables that are only current and voltage. The problem is encountered at low induction motor speeds so that the estimator performance is not good. Therefore, the development of a sensorless system is quite challenging research.

The most popular observer is the Luenberger observer and its derivations as in [2]–[4]. Luenberger observer is arranged by using nextended state-space model that uses an additional state variable. Compared to the Kalman filter as in [5]–[8], this observer requires a lighter computational load [9]. Another group of observers uses artificial intelligence methods such as fuzzy logic or neural networks [10]–[13] and model reference adaptive systems (MRAS) [14]–[17]. According to Morawiec [18], a control theory approach based on the separation of new variables on control objects is proposed. In this case, the extended state-space method described in [2], [3] is used together with the adaptive backstepping method in designing an observer referred to as a Z-type adaptive observer.

The extended state-space has been used in [2], [3], which treats new (additional) variables as disturbances. In this research, the multiplication between rotor speed and rotor flux is treated as a disturbance signal in the induction motor model. The dynamic equation for the exact disturbance is added to the observer structure. This method causes an additional number of observers gains to be determined. Moreover, there is also an additional gain parameter in the adaptation law equation which is used to estimate the speed value. Thus, this method requires more estimator gains. This method is applied to the controller in [19], and implemented in real time in [20].

The use of a disturbance observer which is integrated with the control algorithm has been proposed in [21]. The algorithm for the estimation of the rotor speed is obtained from the disturbance used in the current control loop. The adaptation law derived from the disturbance observer is used to estimate the rotor speed. The principle used is that the observer's results are used in the control law as a feedforward action that aims to mitigate the coupling between the d-q axes. Thus, the performance of the observer depends on the performance of the controller. In other words, the performance of the observer is not independent.

This paper focuses on the extended state-space approach which is used to improve the disturbance observer technique in estimating the induction motor state variables (current and flux) and then speed more easily. In this case, the separation principle in control theory can be applied, so that the observer is independent of the controller. Furthermore, this approach can be applied to a wide operating speed range so that the nonlinearity problem stated in [22], [23] can be handled. Another advantage proposed is that the number of observer gains determined is not too large and the determination is carried out systematically using the principle of duality of observer and controller as described in [24].

2. BASIS OF EXTENDED STATE OBSERVER

The main idea of the extended state observer (ESO) is to combine disturbance signals as additional state variables of the system so that an extended state variable vector is obtained. A simultaneous estimation is carried out with an observer for the extended system. Estimation of disturbance and state variables is carried out in one design, as long as the robustness and boundness conditions are fulfilled.

A linear time-invariant (LTI) system with disturbances in the input and output sections is given as (1) and (2):

$$\dot{x}(t) = Ax(t) + Bu(t) + D_x f_x(t) \tag{1}$$

$$y(t) = Cx(t) + D_y f_y(t) \tag{2}$$

With $x(t) \in \Re^n$, $u(t) \in \Re^m$, $y(t) \in \Re^p$, $f_x(t) \in \Re^r$, $f_y(t) \in \Re^q$ are vectors of states, inputs, measurement outputs, input disturbance, output disturbance (measurement noise), respectively. A, B, C, D_x, D_y are constant real matrices with appropriate dimensions. It is assumed that the pair (A, C) is observable. To shorten the writing, all variables that depend on time are written without using t. We introduce the new state vector $x_z \in R^p$ as (3):

$$\dot{x}_z = A_z(y - x_z) = -A_z x_z + A_z Cx + A_z D_y f_y \tag{3}$$

where A_z is a matrix with the appropriate dimensions. By defining an augmented state X as $X = [x\ x_z]^T$, then we get the new state-space equation – called augmented state equation – from (1) and (3), i.e:

$$\begin{cases} \dot{X} = A_a X + B_a u + E_a f \\ Y = C_a X \end{cases} \tag{4}$$

with

$$A_a = \begin{bmatrix} A & O \\ A_z C & -A_z \end{bmatrix}; \quad B_a = \begin{bmatrix} B \\ O \end{bmatrix}; E_a = \begin{bmatrix} D_d & O \\ O & A_z D_\omega \end{bmatrix}; \quad f = \begin{bmatrix} f_x \\ f_y \end{bmatrix}; C_a = \begin{bmatrix} O & I \end{bmatrix}$$

I and *O* are an identity matrix and a null matrix with appropriate dimensions. From (4), it can be concluded that the transformation of the LTI system model into an augmented state equation causes noise not to appear in the equation of output *Y*, yet appears in the equation of state variable *X*. In other words, output *Y* is free from noise, so it allows an estimation process without noise amplification, even though the estimation equation still uses the multiplication of observer gain with the output variable *Y*.

An observer with proportional-integral (PI) structure can be obtained from the augmented state (4), in the form of as (5):

$$\begin{cases} \dot{\hat{X}} = A_a \hat{X} + B_a u + E_a \hat{f} + L_X (Y - \hat{Y}) \\ \dot{\hat{f}} = L_f (Y - \hat{Y}) \\ \hat{Y} = C_a \hat{X} \end{cases} \tag{5}$$

With $\hat{X}, \hat{f}, \hat{Y}$ are the estimation result of the augmented state, the disturbance, and the output. In (5), the second line explains an integral loop added to the first line, beside the proportional loop. Therefore, this type of observer is called a PI observer, with a structure as shown in Figure 1. L_X is the proportional gain of the observer and L_f is the integral gain of the observer, both of which need to be determined. These observer gains are used to ensure the dynamic stability of the estimation error. Denoted $e_X = X - \hat{X}, e_f = f - \hat{f}$. The dynamics of the PI observer error for system (5) is (6):

$$\begin{cases} \dot{e}_x = (A_a - L_x C_a) e_x + E_a e_f \\ \dot{e}_f = -L_f C_a e_x + \dot{f} \end{cases} \tag{6}$$

or can be written in a more concise form as (7):

$$\dot{\tilde{e}} = (\tilde{A}_a - \tilde{L}\tilde{C}_a)\tilde{e} + \tilde{B}_d \dot{f} \tag{7}$$

with

$$\tilde{e} = \begin{bmatrix} e_X \\ e_{f_a} \end{bmatrix}, \tilde{A}_a = \begin{bmatrix} A_a & E_a \\ O & O \end{bmatrix}, \tilde{L} = \begin{bmatrix} L_X \\ L_f \end{bmatrix}, \tilde{C}_a = \begin{bmatrix} C_a & O \end{bmatrix}, \tilde{B}_d = \begin{bmatrix} O \\ I \end{bmatrix}$$

To estimate the system state accurately, the problem to be solved is to calculate the observer gain $\tilde{L}$ so that the dynamics of observer error $\tilde{e}$ is getting closer to zero. The determination of observer gain can be done through several methods, such as pole placement and linear quadratic regulator (LQR) technique. In (5) may be realized if these conditions are fulfilled:

R1. rank(C) ≥ $r + q$

R2. rank($C.D_x$) ≥ r

R3. rank(obs($\tilde{A}_a, \tilde{C}_a$)) = dim($\tilde{A}_a$)

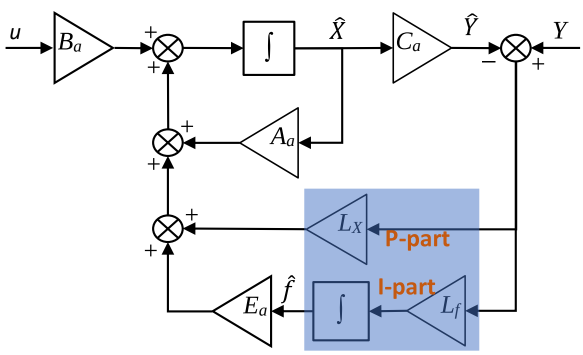

Figure 1. The structure of ESO

It should be noted that (5) is the ESO equation for systems (1) and (2), where there are disturbances at both input and output. If there is only input disturbance, then (5) remains valid by only changing the augmented state (4) to the original state-space (1) and (2). This case occurs in induction motors as described in the next section.

3. NEW DISTURBANCE OBSERVER FOR INDUCTION MOTOR

The state-space model of an induction motor using a stator reference frame is nonlinear one, it is written as (8):

$$\begin{cases} \dot{x}_{IM} = A(x_{IM})x_{IM} + Bu \\ y = Cx_{IM} \end{cases} \tag{8}$$

with $x_{IM} \in \Re^{5\times1}$ and $u \in \Re^{2\times1}$ defined as:

$$x = \begin{bmatrix} i_{ds} \\ i_{qs} \\ \varphi_{dr} \\ \varphi_{qr} \\ \omega_r \end{bmatrix} = \begin{bmatrix} x_1 \\ x_2 \\ x_3 \\ x_4 \\ x_5 \end{bmatrix}; u = \begin{bmatrix} v_{ds} \\ v_{qs} \end{bmatrix}$$

where i_{ds}, i_{qs} are stator currents; and φ_{dr}, φ_{dr} are rotor fluxes in dq axes respectively; while ω_r is the rotor speed.

The matrix $A \in \Re^{5\times5}$ is a function of the rotor speed and the rotor fluxes, whereas the matrix $B \in \Re^{5\times2}$ is a constant. They are formulated as:

$$A = \begin{bmatrix} -A_1 & 0 & A_2 & A_3\omega_r & 0 \\ 0 & -A_1 & -A_3\omega_r & A_2 & 0 \\ A_4 & 0 & -A_5 & -p\dfrac{\omega_r}{2} & 0 \\ 0 & A_4 & -p\dfrac{\omega_r}{2} & -A_5 & 0 \\ -A_6\varphi_{dr} & A_6\varphi_{qr} & 0 & 0 & 0 \end{bmatrix} B = \begin{bmatrix} B_1 & 0 \\ 0 & B_1 \\ 0 & 0 \\ 0 & 0 \\ 0 & 0 \end{bmatrix}$$

with

$$\sigma = 1 - \frac{L_m^2}{L_r\, L_s} \qquad A_1 = \frac{{L_m}^2 R_r + {L_r}^2 R_s}{\sigma\, {L_r}^2\, L_s} \qquad A_2 = \frac{L_m\, R_r}{\sigma\, {L_r}^2\, L_s} \qquad A_3 = \frac{p\, L_m}{2\,\sigma\, L_r\, L_s}$$

$$A_4 = \frac{L_m\, R_r}{L_r} \qquad A_5 = \frac{R_r}{L_r} \qquad A_6 = \frac{p\, L_m}{3\, L_r} \qquad B_1 = \frac{1}{\sigma\, L_s}$$

And symbols that represent the parameters of the induction motor have been described in Table 1. The measured state is only the stator current. Hence, the output matrix $C \in \Re^{2\times5}$ is defined as follows:

$$C = \begin{bmatrix} 1 & 0 & 0 & 0 & 0 \\ 0 & 1 & 0 & 0 & 0 \end{bmatrix}$$

A disturbance observer is a modification of the Luenberger observer with additional state vector *d* that is referred to as disturbance. The matrix *A*, which is the state function, is transformed into a constant matrix by removing the multiplication of rotor speed and flux so that the induction motor state equation becomes as (9):

$$\begin{bmatrix} \dot{i}_{ds} \\ \dot{i}_{qs} \\ \dot{\varphi}_{dr} \\ \dot{\varphi}_{qr} \end{bmatrix} = \begin{bmatrix} -A_1 & 0 & A_2 & 0 \\ 0 & -A_1 & 0 & A_2 \\ A_4 & 0 & -A_5 & 0 \\ 0 & A_4 & 0 & -A_5 \end{bmatrix} \begin{bmatrix} i_{ds} \\ i_{qs} \\ \varphi_{dr} \\ \varphi_{qr} \end{bmatrix} + \begin{bmatrix} A_3 & 0 \\ 0 & -A_3 \\ -\frac{p}{2} & 0 \\ 0 & \frac{p}{2} \end{bmatrix} \begin{bmatrix} d_q \\ d_r \end{bmatrix} + \begin{bmatrix} B_1 & 0 \\ 0 & B_1 \\ 0 & 0 \\ 0 & 0 \end{bmatrix} \begin{bmatrix} v_{ds} \\ v_{qs} \end{bmatrix} \tag{9}$$

with

$$\begin{cases} d_d = \omega_r \varphi_{qr} \\ d_q = \omega_r \varphi_{dr} \end{cases} \tag{10}$$

or to be written in a more concise form as (11):

$$\dot{x} = Ax + Bu + D_d d \tag{11}$$

with

$$x = \begin{bmatrix} i_{ds} \\ i_{qs} \\ \varphi_{dr} \\ \varphi_{qr} \end{bmatrix}, d = \begin{bmatrix} d_d \\ d_q \end{bmatrix}, A = \begin{bmatrix} -A_1 & 0 & A_2 & 0 \\ 0 & -A_1 & 0 & A_2 \\ A_4 & 0 & -A_5 & 0 \\ 0 & A_4 & 0 & -A_5 \end{bmatrix}, D_d = \begin{bmatrix} A_3 & 0 \\ 0 & -A_3 \\ -\frac{p}{2} & 0 \\ 0 & \frac{p}{2} \end{bmatrix}, B = \begin{bmatrix} B_1 & 0 \\ 0 & B_1 \\ 0 & 0 \\ 0 & 0 \end{bmatrix}$$

It should be noted that the nonlinear dynamics from the induction motor in (8) has been already shown in (11), which has a linear dynamic model structure such as (1). Here, d is the input disturbance notated f_x in (1). If assumed the dynamics of change in d is very small, then $d = 0$. Next, (11) can be rewritten as follows:

$$\begin{bmatrix} \dot{x} \\ \dot{d} \end{bmatrix} = \begin{bmatrix} A & D_d \\ O & O \end{bmatrix} \begin{bmatrix} x \\ d \end{bmatrix} + \begin{bmatrix} B \\ O \end{bmatrix} v \tag{12}$$

or can be written in a more concise form to obtain an extended state-space equation, i.e.:

$$\dot{x_a} = A_a x_a + B_a u \tag{13}$$

with

$$x_a = \begin{bmatrix} x \\ d \end{bmatrix}, A_a = \begin{bmatrix} A & D_d \\ 0 & 0 \end{bmatrix}, B_a = \begin{bmatrix} B \\ 0 \end{bmatrix}$$

The disturbance observer algorithm is derived by referring to (13), which is written as (15):

$$\dot{\hat{x}}_a = A_a \hat{x}_a + B_a u + L(i_s - \hat{\imath}_s) \tag{14}$$

$$\hat{y} = \begin{bmatrix} C & O \\ O & I \end{bmatrix} \begin{bmatrix} x \\ d \end{bmatrix} = C_a x_a \tag{15}$$

Notice that (14) – (15) are the compact form of (5).

The observer gain L is determined through the LQR method to avoid a time-consuming trial and error. In the LQR method, the matrix $Q \in \Re^{6x6}$ and $\Re \in R^{4x4}$ are needed to find the value of L with optimization techniques. To avoid singularity, the matrix A_a needs to be written in (16):

$$A_a = \begin{bmatrix} A & D_d \\ 0 & \varepsilon I \end{bmatrix} \tag{16}$$

with ε is a very small real number. The results of the disturbance and flux estimation are then used to estimate the value of the rotor speed using as (17):

$$\hat{\omega}_r = \frac{\hat{d}^T \hat{\varphi}}{|\hat{d}^T \hat{\varphi}|} \sqrt{\frac{|\hat{d}|^2}{|\hat{\varphi}|^2}} \tag{17}$$

with

$$|\hat{d}| = \sqrt{\hat{d}_d^2 + \hat{d}_q^2}\ ; |\hat{\varphi}| = \sqrt{\hat{\varphi}_{dr}^2 + \hat{\varphi}_{qr}^2}$$

In addition, the current and flux estimation results can be used to estimate the motor electromagnetic torque value T_e using as (18):

$$\hat{T}_e = 3\frac{L_m}{L_r}\left(\hat{\varphi}_{dr}\hat{i}_{qs} - \hat{\varphi}_{qr}\hat{i}_{ds}\right) \quad (18)$$

The improvement of the estimator algorithm in Figure 2 offers the advantage of a simpler structure with a systematically determined observer gain. Unlike in the previous disturbance observer algorithm where the adaptation law was still used, in this modified disturbance observer, the adaptation law is no longer used. This observer is then referred to as an ESO.

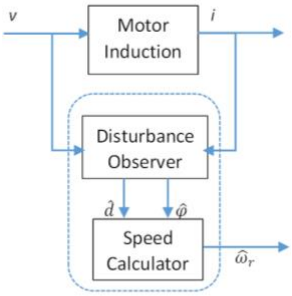

Figure 2. The speed estimator with ESO algorithm-based disturbance observer

4. DISCRETE FORM OF THE ESTIMATOR

The application of the estimator algorithm in real-time with a computer/microcontroller needs a discrete-time approach. Therefore, the estimator algorithm is required to be expressed in the discrete-time domain or also known as the discrete-time estimator. In this case, the new disturbance observer also needs to be expressed in the form of a discrete-time observer.

The representation of the new discrete-time disturbance observer is as (19) and (20):

$$\dot{\hat{x}}_a(k+1) = F_a\hat{x}_a(k) + G_a u(k) + \Lambda\left(i_s(k) - \hat{i}_s(k)\right) \quad (19)$$

$$\hat{y}(k) = C_a\hat{x}_a(k) \quad (20)$$

with k representing the time index, and F_a, G_a is the discrete forms of A_a and B_a, which can be determined through in (21) and (22):

$$F_a = (I + A_a T_s) \quad (21)$$

$$G_a = B_a T_s \quad (22)$$

with T_s as sampling time. The determination of discrete observer gain, Λ, can be done using the discrete LQR method.

5. SIMULATION RESULTS

The performance of the estimator proposed in this paper is tested by numerical simulation. The parameters of the induction motor model used in the simulation are shown in Table 1. The tests were carried out for both the continuous observer and the discrete observer.

5.1. The continues observer

The noise power from measurement for both current and voltage was 10^{-6}. In the high-speed test, the induction motor was loaded with a torque of 11.9 Nm at the start-up stage. Here, there are two test scenarios carried out, i.e., change in speed command and change in load torque command. The values of Q and R used to determine the continuous observer gain were:

$$Q = \begin{bmatrix} 0.1I & O & O \\ O & 0.1I & O \\ O & O & 10^{11}I \end{bmatrix}, R = 0.1I$$

The scenario of change in rotor speed was started at 0.8 seconds, i.e., from 361 rad/s (1 p.u.) to -216 rad/s (-0.6 p.u.). The negative value indicates that the motor rotated in a reverse direction. This scenario represents a field-weakening phenomenon. The test result is shown in Figure 3. It can be observed that the results of the estimated speed and magnitude of the rotor flux and stator current are close to their true values. The speed estimation error is only seen when the field weakening is shown by the arrow. At that time, changes in the magnitude of the rotor flux are quite large. Nevertheless, the proposed continuous observer can overcome this change quite well so that the estimated flux rotor and current are close to the true values. The oscillating current value is denser than the value of the flux and still can be estimated accurately as shown in the zoomed stator current graph.

Table 1. Parameters of the induction motor used

Parameter	Symbol	Value
Rated power	P_{nom}	3 kW
Rated speed	ω_{nom}	361.1 rad/s
Voltage (line-line)	V_n	220 volt rms
Frequency	f	60 Hz
Mutual inductance	L_m	0.069 H
Rotor inductance	L_r	0.071 H
Stator inductance	L_s	0.073 H
Rotor resistance	R_r	0.816 Ohm
Stator resistance	R_s	0.435 Ohm
Rotor inertia	J	0.089 kg.m^2
Number of pole	p	4

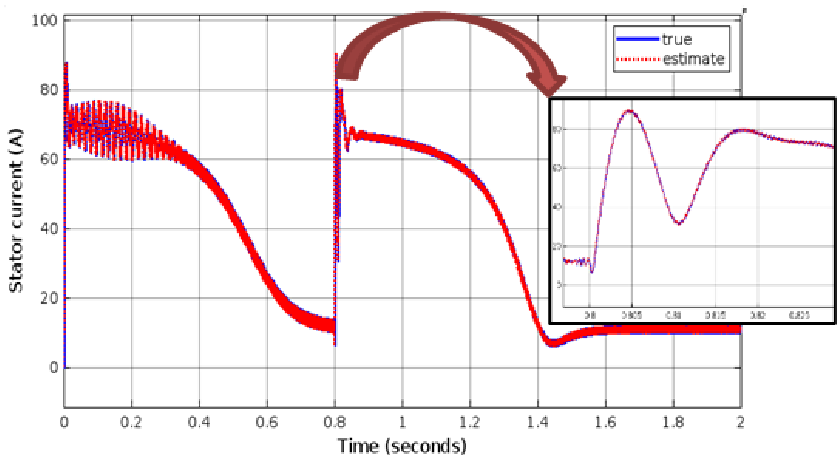

Figure 3. The test result of the proposed continuous observer when field weakening occurs

The load torque change test is shown in Figure 4. The load changed from 11.9 Nm to 30 Nm at 1 second as shown by the arrow. The load addition caused the speed to drop because there was no feedback control here. The results of this test prove that the proposed estimator can handle changes in load torque so that the estimated rotor speed is still in line with its true value. Moreover, this estimator can estimate the electromagnetic torque accurately as shown in the zoomed version of the electromagnetic torque graph.

The proposed continuous observer was also tested for induction motor operation at low speed and without load torque (idle run condition). The change in rotor speed from 7.2 rad/s (0.02 p.u.) to -3.7 rad/s (-0.01 p.u.) occurred at 1.8 seconds. The estimation result for this case is shown in Figure 5. It is shown that although its performance is not as good as at high speeds, the estimator can still estimate the rotor speed with the root mean square (RMS) value of the residual speed of about 0.1. The state estimation results by the observer, both rotor flux and stator current, are close to the true value. The results of the stator current measurement, which has a noise power of 10^{-6}, are almost the same as the estimated result. The error of the estimator at low speed is caused by the noise in the voltage measurement. It can be concluded that the observer performance at low speed depends on the measurement noise value because of the small voltage value in this operation.

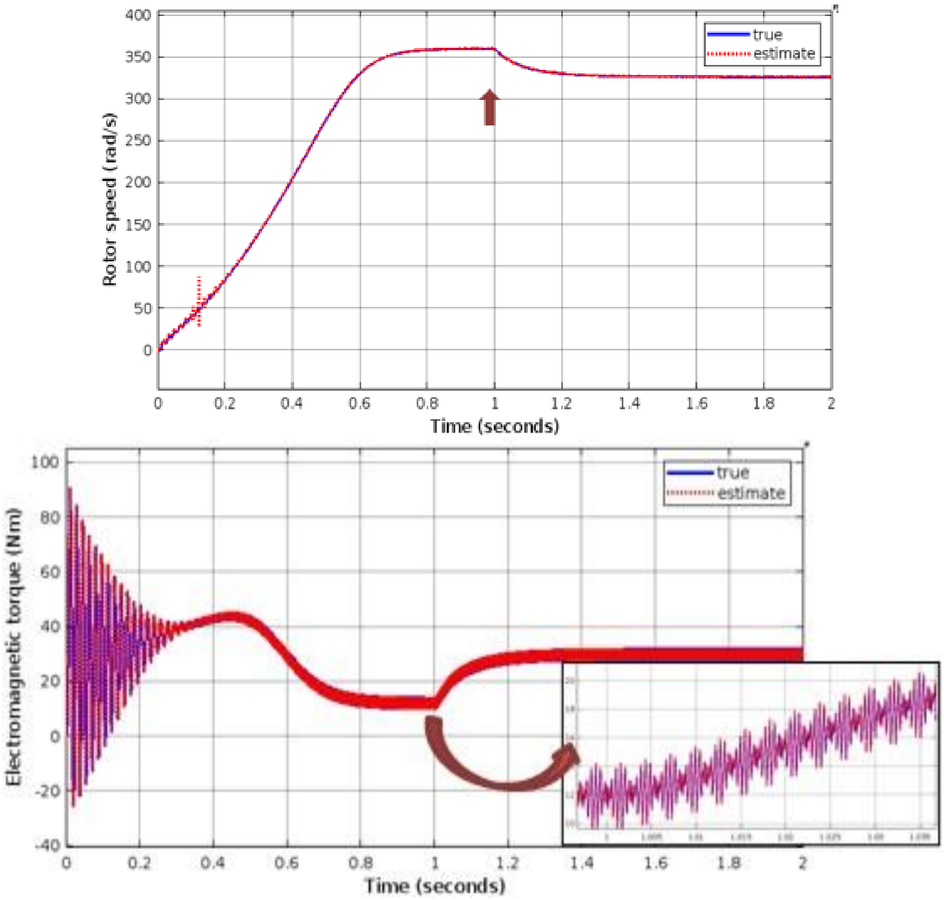

Figure 4. The test result of the proposed continuous observer when changes in load

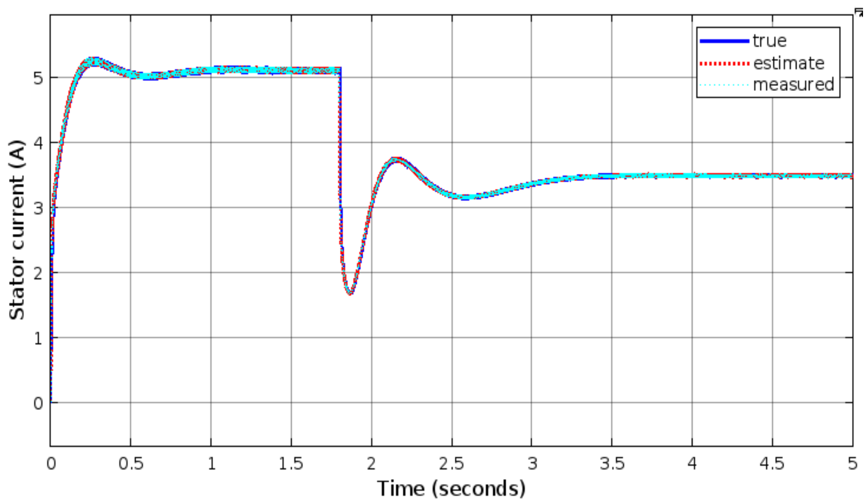

Figure 5. The test result of the proposed discrete observer at low speed

Further, the comparative values of speed estimates under no-load condition for different speed estimation techniques namely improved adaptive extended Kalman filter (IEKF) and MRAS reported in [25] as well as the proposed estimator are presented in Table 2. These results confirm that the capability of the proposed estimator in estimating the rotor speed of induction motor over a wide speed range demanded are better than other techniques. Although IEKF is able to estimate at high speed while MRAS is not, its estimation error is larger than the proposed estimator one. The proposed estimator has a lower RMSE value, that is 60.75% of the RMSE value of IEKF.

Table 2. Parameters of the induction motor used

Speed demand (rad/s)	MRAS results (rad/s)	IEKF results (rad/s)	The proposed estimator results (rad/s)
30	29.6	29.87	29.98
60	59.42	59.76	60.10
100	98.67	99.02	100.30
120	*not achieved*	119.23	120
139	*not achieved*	138.75	138.60

5.2. The discrete oberver

The discrete observer test was carried out in three cases: first, the load change test and the speed command at the same time; second, measurement noise test; third, motor parameter uncertainty test. The last two test scenarios are intended to represent technical things when implementing the estimator in real time. The values of Q and R used to determine the discrete observer gain were.

$$Q = \begin{bmatrix} 0.1I & O & O \\ O & 10^{-6}I & O \\ O & O & 10^{5}I \end{bmatrix}, R = 0.1I$$

The first test was carried out to determine the ability of the discrete observer in handling changes in speed and load torque. As with the continuous observer testing, the measurement noise for both current and voltage has a noise power of 10^{-6} and the induction motor is loaded with a torque of 11.9 Nm at the start-up stage. The test results are shown in Figure 6. When there is a change in load (to 30 Nm), which causes the speed to decrease, and when there is a change in the speed command (from 1 p.u. to -0.6 p.u.), it is shown that the estimator can estimate of the speed and electromagnetic torque according to their true values. In addition, the discrete observer can also estimate the stator current and rotor flux that are close to their true values, as shown in the zoomed graph.

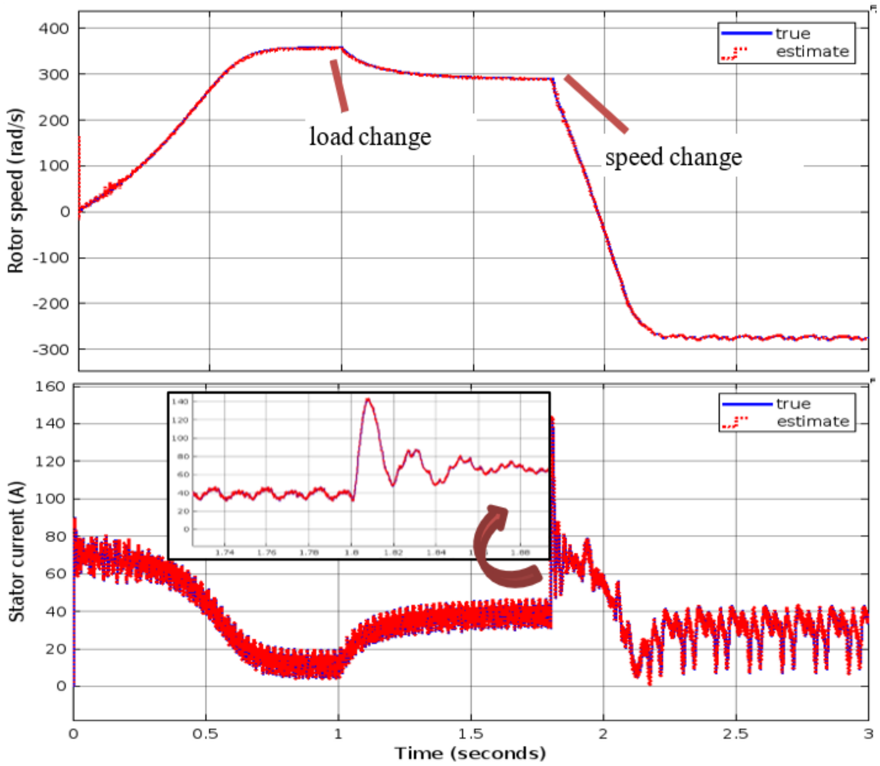

Figure 6. The test result of the proposed discrete observer when changes in load and speed occur

The noise test was carried out by varying the noise power of the voltage and current measurements. Variations are given in three values, i.e., 10^{-4}, 10^{-3}; and 10^{-2}. The voltage measurement noise test result is shown in Figure 7, while the current measurement noise test result is shown in Figure 8. It is shown that the voltage measurement noise affects the rotor speed estimation results more significantly than the current measurement noise. This result is in line with the results of the continuous observer test in the explanation above. The greater the voltage measurement noise, the greater the RMS value of the rotor speed residual as shown in Figure 7. On the contrary, the current measurement noise only causes a small offset in the estimated speed as shown by the zoomed rotor speed graph in Figure 8. The gain observer used in this simulation is determined by using the LQR method. If the measurement noise is large, the observer gain can be determined using the linear quadratic Gaussian (LQG) method. This method is quite easy to do considering that no changes are made to the observer equation. Only noise information needs to be added to apply the LQG method.

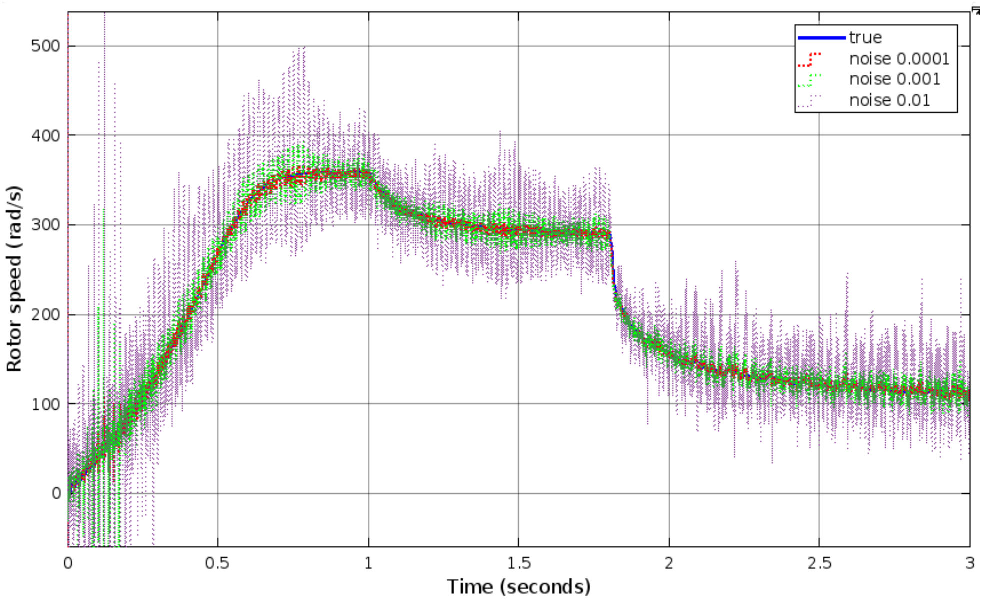

Figure 7. The test results of the proposed discrete observer for three variations of current noise

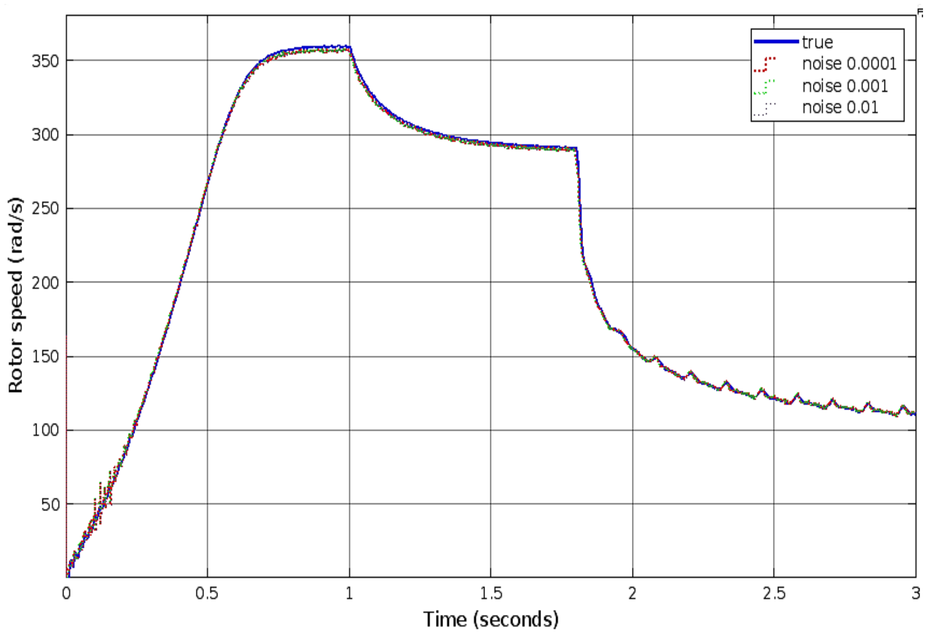

Figure 8. The test results of the proposed discrete observer for three variations of voltage noise

The motor parameter uncertainty test is carried out by varying the value of the stator resistance and the mutual inductance value in the induction motor model. Each parameter is varied by two values, i.e., 5% and 10% of the nominal value for the stator resistance parameter; and 0.1% and 0.2% of nominal values for mutual inductance parameters. The results of the parameter uncertainty test are shown in Figure 9 for the variation of the stator resistance parameter, and in Figure 10 for the variation of the mutual inductance parameter. The impact of the uncertainty of the parameters of the induction motor model is that the estimated results of the rotor speed oscillate residual. The greater the uncertainty, the greater the RMS value. In addition, it is also shown that the uncertainty of the inductance model has a worse impact and greater oscillation frequency than the uncertainty of the stator resistance model. The results of this test prove that the observer proposed in this study is robust to the uncertainty of the parameters of the induction motor model to a certain level. Although oscillating, overall, the estimation results tend to follow the true value. The mean value of this oscillation is close to its true value. This information can be used as the basis for improving the estimator algorithm in further research so that the problem of uncertainty in the parameters of the induction motor model can be resolved. As in the noise test, the LQG method to determine observer gain might be tried to improve the estimation results.

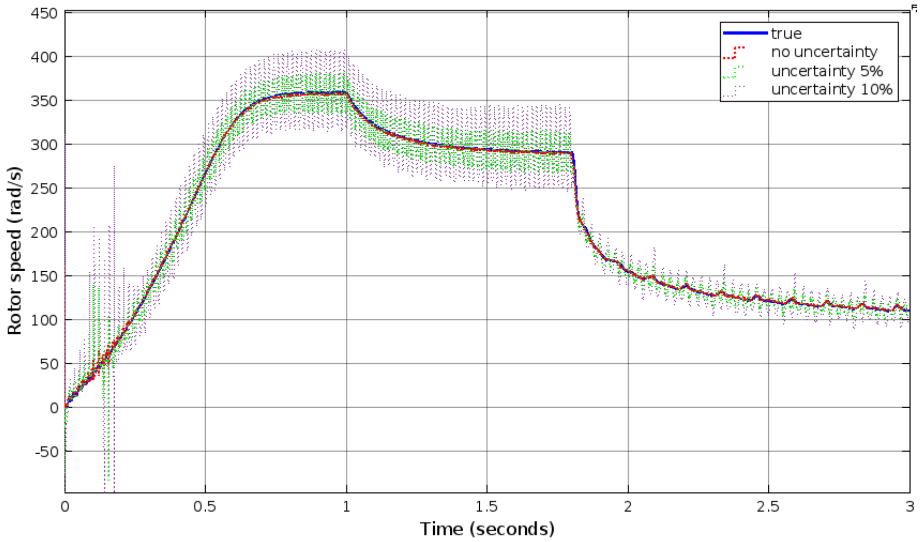

Figure 9. The test result of the proposed discrete observer for two variations of stator resistance value

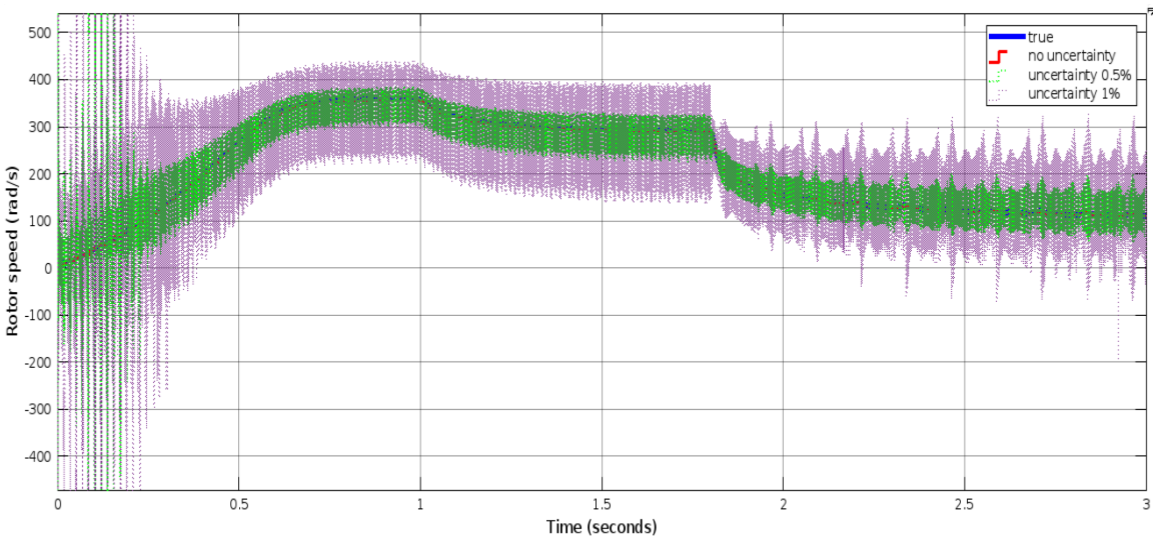

Figure 10. The test result of the proposed discrete observer for two variations of mutual inductance value

6. CONCLUSION

The proposed new disturbance observer guarantees the correct result of the speed estimator for a wide range of induction motor operation. Its simple structure is proven to overcome the nonlinearity problem of the induction motor. The test results show that this observer is also able to operate well in conditions of field weakening and load changes. The proposed discrete observer has been tested for implementation purposes, where it is found that the influence of noise and the uncertainty of the induction motor model parameters can be solved at a certain level. The improvement of the observer to increase its robustness can be a challenging research topic. The observer application for speed sensorless drives for induction motors in real-time is also potential for further research.

ACKNOWLEDGEMENTS

This work was supported by the Directorate of Research, Technology and Community Service/ Ministry of Education, Culture, Research and Technology, under Basic Research Grant (reference 1512/PKS/ITS/2022).

REFERENCES

[1] M. S. Zaky, M. Khater, H. Yasin, and S. S. Shokralla, "Review of different speed estimation schemes for sensorless induction motor drives," *Journal of Electrical Engineering*, vol. 8, no. 2, pp. 39–39, 2008.

[2] Z. Krzemiński, "Observer of induction motor speed based on exact disturbance model," in *2008 13th International Power Electronics and Motion Control Conference, EPE-PEMC 2008*, IEEE, Sep. 2008, pp. 2294–2299, doi: 10.1109/EPEPEMC.2008.4635605.

[3] Z. Krzemiński, A. Lewicki, and M. Morawiec, "Speed observer based on extended model of induction machine," in *IEEE International Symposium on Industrial Electronics*, IEEE, 2010, pp. 3107–3112, doi: 10.1109/ISIE.2010.5637685.

[4] J. You, W. Wu, and Y. Wang, "An adaptive luenberger observer for speed-sensorless estimation of induction machines," in *Proceedings of the American Control Conference*, IEEE, 2018, pp. 307–312, doi: 10.23919/ACC.2018.8431006.

[5] Y. Zahraoui and M. Akherraz, "Kalman filtering applied to induction motor state estimation," in *Dynamic Data Assimilation - Beating the Uncertainties*, IntechOpen, 2020, doi: 10.5772/intechopen.92871.

[6] S. Jafarzadeh, C. Lascu, and M. S. Fadali, "State estimation of induction motor drives using the unscented Kalman filter," *IEEE Transactions on Industrial Electronics*, vol. 59, no. 11, pp. 4207–4216, Nov. 2012, doi: 10.1109/TIE.2011.2174533.

[7] L. Et-Taaj, Z. Boulghasoul, A. Elbacha, and A. El Kharki, "Robust sensorless induction motor control based on extended Kalman filter observer," in *2021 International Congress of Advanced Technology and Engineering, ICOTEN 2021*, IEEE, 2021, doi: 10.1109/ICOTEN52080.2021.9493502.

[8] P. Mercorelli, "A hysteresis hybrid extended kalman filter as an observer for sensorless valve control in camless internal combustion engines," *IEEE Transactions on Industry Applications*, vol. 48, no. 6, pp. 1940–1949, Nov. 2012, doi: 10.1109/TIA.2012.2226193.

[9] Y. Zhang, Z. Zhao, T. Lu, L. Yuan, W. Xu, and J. Zhu, "A comparative study of luenberger observer, sliding mode observer and extended Kalman filter for sensorless vector control of induction motor drives," in *2009 IEEE Energy Conversion Congress and Exposition, ECCE 2009*, IEEE, Sep. 2009, pp. 2466–2473, doi: 10.1109/ECCE.2009.5316508.

[10] N. Pimkumwong and M. S. Wang, "Online speed estimation using artificial neural network for speed sensorless direct torque control of induction motor based on constant V/F control technique," *Energies*, vol. 11, no. 8, 2018, doi: 10.3390/en11082176.

[11] T. H. D. Santos, I. N. D. Silva, A. Goedtel, and M. F. Castoldi, "Neural speed estimation applied to stator flux-oriented control drives," *Electric Power Components and Systems*, vol. 47, no. 9–10, pp. 798–809, 2019, doi: 10.1080/15325008.2019.1627613.

[12] M. M. Hasan, "Artificial neural network based speed estimator for sensorless field oriented control of three phase induction motor," in *3rd International Conference on Electrical, Computer and Telecommunication Engineering, ICECTE 2019*, IEEE, 2019, pp. 57–60, doi: 10.1109/ICECTE48615.2019.9303559.

[13] S. N. Mahsahirun, N. R. N. Idris, Z. M. Yusof, and T. Sutikno, "Non-parametric induction motor rotor flux estimator based on feed-forward neural network," *International Journal of Power Electronics and Drive Systems*, vol. 13, no. 2, pp. 1229–1237, 2022, doi: 10.11591/ijpeds.v13.i2.pp1229-1237.

[14] M. Korzonek, G. Tarchala, and T. O. -Kowalska, "A review on MRAS-type speed estimators for reliable and efficient induction motor drives," *ISA Transactions*, vol. 93, pp. 1–13, 2019, doi: 10.1016/j.isatra.2019.03.022.

[15] T. O. -Kowalska, M. Korzonek, and G. Tarchala, "Performance analysis of speed-sensorless induction motor drive using discrete current-error based mras estimators," *Energies*, vol. 13, no. 10, 2020, doi: 10.3390/en13102595.

[16] W. E. Merrassi, A. Abounada, and M. Ramzi, "Advanced speed sensorless control strategy for induction machine based on neuro-MRAS observer," *Materials Today: Proceedings*, vol. 45, pp. 7616–7621, 2021, doi: 10.1016/j.matpr.2021.03.081.

[17] P. Misra and B. Kumar, "Rotor resistance estimation for improved performance of MRAS-based sensorless speed estimation of induction motor drives," in *Algorithms for Intelligent Systems*, Springer Singapore, 2021, pp. 177–187, doi: 10.1007/978-981-15-8045-1_18.

[18] M. Morawiec, "Z-type observer backstepping for induction machines," *IEEE Transactions on Industrial Electronics*, vol. 62, no. 4, pp. 2090–2102, Apr. 2014, doi: 10.1109/TIE.2014.2355417.

[19] K. Indriawati, B. L. Widjiantoro, and N. R. I. Rachman, "Disturbance observer-based speed estimator for controlling speed sensorless induction motor," in *2020 3rd International Seminar on Research of Information Technology and Intelligent Systems, ISRITI 2020*, IEEE, 2020, pp. 301–305, doi: 10.1109/ISRITI51436.2020.9315387.

[20] K. Indriawati, F. P. Wijaya, and C. Mufit, "Implementation of disturbance observer for sensorless speed estimation in induction motor," *International Journal of Power Electronics and Drive Systems*, vol. 13, no. 2, pp. 724–732, 2022, doi: 10.11591/ijpeds.v13.i2.pp724-732.

[21] T. Gabbi, C. Osoorio, C. Volpato, D. Dotto, H. Grundling, and R. Vieira, "Speed estimation algorithm of induction motors based on disturbance observer," in *2017 IEEE International Electric Machines and Drives Conference, IEMDC 2017*, IEEE, 2017, pp. 1–6, doi: 10.1109/IEMDC.2017.8002216.

[22] K. Blecharz, D. Wachowiak, and Z. Krzemiski, "A novel speed observer for doubly-fed induction generator," in *2017 19th European Conference on Power Electronics and Applications, EPE 2017 ECCE Europe*, IEEE, Sep. 2017, doi: 10.23919/EPE17ECCEEurope.2017.8099137.
[23] T. Bialon, M. Pasko, and R. Niestrój, "Developing induction motor state observers with increased robustness," *Energies*, vol. 13, no. 20, 2020, doi: 10.3390/en13205487.
[24] K. Indriawati, T. Agustinah, and A. Jazidie, "Development of the PD/PI extended state observer to detect sensor and actuator faults simultaneously," *International Conference on Electrical Engineering, Computer Science and Informatics (EECSI)*, vol. 2, no. 1, pp. 165–171, 2015, doi: 10.11591/eecsi.v2i1.801.
[25] M. L. Jayaramu, H. N. Suresh, M. S. Bhaskar, D. Almakhles, S. Padmanaban, and U. Subramaniam, "Real-time implementation of extended kalman filter observer with improved speed estimation for sensorless control," *IEEE Access*, vol. 9, pp. 50452–50465, 2021, doi: 10.1109/ACCESS.2021.3069676.

BIOGRAPHIES OF AUTHORS

Katherin Indriawati received the B.Eng. degree in engineering physics and the M. Eng degree in instrumentation & control, from Institut Teknologi Bandung (ITB), Bandung, Indonesia, in 1998 and 2005, respectively. She has taken the Ph.D. degree at Institut Teknologi Sepuluh November (ITS), Surabaya, Indonesia. Since 2014, she has been an Assistant Professor with the Department of Engineering Physics, ITS. She is the author of more than 50 articles. Her research interests include supervisory control, fault tolerant control, fault detection, diagnosis and decision-making scheme. She can be contacted at email: katherin@ep.its.ac.id.

Febry Pandu Wijaya received the B.Eng. degree in electical engineering from the Institut Teknologi Bandung, Bandung, Indonesia, in 2006, the M.Eng. degree in mechanical engineering from Toyohashi University of Technology, Toyohashi, Japan, in 2014, and the Ph.D. degree in electrical and electronic engineering from Chiba University, Chiba, Japan, in 2017. Since 2007, he has been with PT INKA (Indonesian Rolling Stock Industry), Madiun, Indonesia. His research interests include induction motor control, railway traction system, hybrid railway vehicle, and electric bus. He can be contacted at email: febry.pwijaya@inka.co.id.

Choirul Mufit received the B.Eng. degree in engineering physics from the Sepuluh Nopember Institute of Technology (ITS), Surabaya, Indonesia, in 2019. has completed a master's degree in engineering physics at Sepuluh Nopember Institute of Technology (ITS), Surabaya, Indonesia in 2021. During college in 2014-2021, he joined as a laboratory assistant at the Physcal Measurement Laboratory of the Department of Engineering Physics, ITS. Now he was Head Electrical Engineering in Universitas 17 agustus 1945 Jakarta. His research interests include reweneble energy, electronic instrumentation, and measurement device. He can be contacted at email:mufitsetiawan@gmail.com.